THE JOURNAL OF BIOLOGICAL CHEMISTRY
Vol. 278, No. 44, Issue of October 31, pp. 42867–42876, 2003
Printed in U.S.A.

Regulation of a TRPM7-like Current in Rat Brain Microglia*

Received for publication, April 29, 2003, and in revised form, August 5, 2003
Published, JBC Papers in Press, August 6, 2003, DOI 10.1074/jbc.M304487200

Xinpo Jiang‡, Evan W. Newell‡§, and Lyanne C. Schlichter‡§¶

From the ‡Division of Cellular and Molecular Biology, Toronto Western Research Institute, 399 Bathurst Street, Toronto, Ontario M5T 2S8, Canada and §Department of Physiology, University of Toronto, Toronto, Ontario M5S 1A8, Canada

Non-excitable cells use Ca^{2+} influx for essential functions but usually lack voltage-gated Ca^{2+} channels. The main routes of Ca^{2+} entry appear to be store-operated channels or Ca^{2+}-permeable non-selective cation channels, of which the magnesium-inhibited cation (or magnesium-nucleotide-regulated metal cation) current has received considerable recent attention. This current appears to be produced by one of the recently cloned transient receptor potential (TRP) channels, TRPM7. In this study of rat microglia, we identified TRPM7 transcripts and a prevalent current with the hallmark biophysical and pharmacological features of TRPM7. This is the first identification of a TRPM7-like current in the brain. There is little known about how members of the TRPM sub-family normally become activated. Using whole-cell patch clamp recordings from rat microglia, we found that the TRPM7-like current activates spontaneously after break-in and that the current and its activation are inhibited by elevated intracellular Mg^{2+} but not affected by cell swelling or a wide range of intracellular Ca^{2+} concentrations. The TRPM7-like current in microglia appears to depend on tyrosine phosphorylation. It was inhibited by several tyrosine kinase inhibitors, including a peptide (Src 40–58) that was shown previously to inhibit Src actions, but not by inactive drugs or peptide analogues. The current did not depend on the cell activation state; *i.e.* it was the same in microglia recently removed from the brain or when cultured under a wide range of conditions that favor the resting or activated state. Because TRPM7 channels are permeable to Ca^{2+}, this current may be important for microglia functions that depend on elevations in intracellular Ca^{2+}.

Non-excitable cells use trans-membrane Ca^{2+} influxes for essential cell functions, including proliferation, apoptosis, secretion, volume regulation, and ion homeostasis. Immune cells were among the first and remain among the most intensively studied, with focus on general and more specific roles of Ca^{2+} signaling, such as mitogenic activation, secretion of lymphokines, cytokines, cytotoxic molecules, and antibodies, and on phagocytosis, respiratory burst, and migration. In parallel, there have been an increasing number of studies on the pathways of Ca^{2+} entry into these cells. In almost all cases, the role of membrane potential in Ca^{2+} influx in non-excitable cells is fundamentally different from excitable cells. Voltage-gated Ca^{2+} channels are rare in immune cells, and many cell types appear to be devoid of them. In these cells, although Ca^{2+} influx is electrogenic and tends to depolarize the cell, the main effect of depolarization is to reduce the driving force for Ca^{2+} influx. Because hyperpolarization favors Ca^{2+} entry, the focus has been on store-operated Ca^{2+} channels, including the Ca^{2+}-release-activated Ca^{2+} (CRAC)[1] channel, and on Ca^{2+}-permeable non-selective cation channels. The CRAC current is widely expressed in immune cells, where it is one of the best characterized store-operated channels (1, 2). However, two Ca^{2+}-permeable channel types often co-exist. Recent studies on the Jurkat T cell line and rat basophilic leukemia cells were the first to distinguish between co-existing CRAC currents and a Mg^{2+}-inhibited cation current (also called magnesium nucleotide-regulated metal cation current) (3–5). The latter current is nearly identical to one of the recently cloned transient receptor potential (TRP) channels, TRPM7.

The TRP family comprises >20 channels, all with six transmembrane domains and cytoplasmic N and C termini, and recently divided into three sub-families: TRPC, TRPV, and TRPM (for reviews see Refs. 6–8). Many of these channels are widely distributed in mammalian tissues, and following their cloning and heterologous expression, properties of some have made them excellent candidates for the Ca^{2+} entry pathways of non-excitable cells. Most members of the TRPC sub-family are store-operated and Ca^{2+} permeable, one of the TRPV members (TRPV4) is activated by changes in cell volume, and some members of the TRPM sub-family (TRPM7, TRPM8) are permeable to divalent cations, including Ca^{2+} (9, 10). TRP channels are not voltage-gated and thus are open over a wide range of voltages once activated. Those that are Ca^{2+}-permeable produce Ca^{2+} influxes that increase with the driving force; *i.e.* with hyperpolarizing membrane potentials, the common feature of Ca^{2+} entry into immune cells and many other non-excitable cells. Indeed, the properties of TRPM7 (9, 11) make it the best candidate for the non-store-operated Ca^{2+} pathway for Ca^{2+} entry in many immune cells.

Expression of TRPM7 is widespread, with transcripts in brain, spleen, lung, kidney, heart, and liver (9, 11). Within the brain, it is not known which cell types express this channel or what role it might play in normal or pathological brain function. We have been studying ion-channel expression and roles in the immune cell of the central nervous system, the microglia. These cells express several types of K^+ channels, and some are involved in key microglia functions; *e.g.* proliferation and the respiratory burst (12, 13), reviewed

* This work was supported in part by grants from the Canadian Institutes for Health Research (MT-13657), the Heart and Stroke Foundation of Ontario (T-3726), and the Natural Sciences and Engineering Research Council (to L. C. S.) and by a scholarship from the National Science Foundation, USA (to E. N.). The costs of publication of this article were defrayed in part by the payment of page charges. This article must therefore be hereby marked "*advertisement*" in accordance with 18 U.S.C. Section 1734 solely to indicate this fact.

¶ To whom correspondence should be addressed. Tel.: 416-603-5970; Fax: 416-603-5745; E-mail: schlicht@uhnres.utoronto.ca.

[1] The abbreviations used are: CRAC, Ca^{2+}-release-activated Ca^{2+}; ACM, astrocyte conditioned medium; 2-APB, 2-aminoethyldiphenyl borate; K_4BAPTA, $K_4$1,2-bis(2-aminophenoxy) ethane *N*,*N*,*N*′,*N*′-tetraacetic acid; MEM, minimal essential medium; nMDG, n-methyl D-glucamine; NPPB, 5-nitro-2-(3-phenylpropylamino)benzoic acid; TRP, transient receptor potential; PLC, phospholipase C.

in Ref. 14. Although the precise roles of the K^+ channels are not yet known, they may act by maintaining a hyperpolarized membrane potential and facilitating Ca^{2+} entry, as in lymphocytes (for reviews see Refs. 14 and 15). The routes of Ca^{2+} entry in microglia are poorly understood. Microglia have ionotropic purinergic receptors that are permeable to Ca^{2+} and monovalent cations (16) and a current reported to be CRAC (17), both of which should produce Ca^{2+} influxes that increase with hyperpolarization. The functional expression of voltage-gated Ca^{2+} channels (18) is somewhat controversial, but if present they should produce a depolarization-activated Ca^{2+} influx. The presence of other Ca^{2+}-permeable channels in microglia has not been reported. In the present study, we have identified transcripts for TRPM7 and characterized a prevalent current in rat brain microglia that has the hallmark features of expressed TRPM7 channels. The same current was expressed in *ex vivo* microglia, studied within 2 days of removal from the brain, as well as in microglia cultured under a wide range of conditions that favor either the resting or activated cell state.

There is little known about how members of the TRPM sub-family normally become activated. For instance, TRPM7 contains an active protein kinase domain (atypical α-kinase), it can phosphorylate itself, and mutations in the ATP-binding motif reduce the current (9). But it appears that effects of changing ATP may be entirely because of inhibition of TRPM7 channel activation by intracellular free Mg^{2+} (10, 11), which is also a distinguishing feature of native Mg^{2+}-inhibited cation or magnesium nucleotide-regulated metal cation currents (3–5; 19). We addressed this question in the present study, using whole-cell and perforated patch clamp recordings on rat microglia. We found that the TRPM7-like current activates spontaneously after break-in, but much less current develops in perforated-patch recordings. The current, like TRPM7, was inhibited by millimolar total intracellular Mg^{2+} concentrations. It was not affected by cell swelling or a wide range of intracellular Ca^{2+} concentrations. Activation of the current was inhibited by several tyrosine kinase inhibitors and by a peptide that interferes with actions of Src kinase but not by the appropriate inactive drug analogues or a scrambled peptide. Because TRPM7 channels are permeable to Ca^{2+}, this current may be important for microglia functions that depend on elevations in intracellular Ca^{2+}.

EXPERIMENTAL PROCEDURES

Microglia—Cultures of highly purified microglia were prepared from neopallia of 2-day-old Wistar rat pups (Charles River, Quebec) as described previously (20). In brief, finely minced neopallial tissue was pelleted and resuspended in minimal essential medium (MEM; University Health Network, Sera and Media Services, Toronto). The tissue was filtered through a 40-μm cell strainer and re-suspended in MEM that was supplemented with 5% horse serum, 5% fetal bovine serum, and 0.05 mg/ml gentamycin (all from Invitrogen). The cells were then seeded into 75-cm^2 flasks and re-fed 2 days after isolation. After 10–12 days in culture without feeding, the flasks were shaken (180 rpm, 8–12 h), and the floating cells (>95% pure microglia) were harvested. For electrophysiology, microglia were plated on 15-mm sterile glass coverslips and cultured in either serum-free medium (*i.e.* MEM with 2% B27 supplement (Invitrogen), 2 mM L-glutamine, and 0.05 mg/ml gentamycin) or astrocyte-conditioned medium (ACM), collected as the supernatant from rat astrocyte cultures grown in MEM with 2% fetal bovine serum (21). ACM was collected twice a week, frozen at −70 °C, and used within one month. Where indicated, microglia were treated with 100 ng/ml lipopolysaccharide or 100 nM phorbol myristate acetate overnight before patch clamping. For *ex vivo* cells, freshly prepared suspensions of neopallial tissue were plated onto 15-mm sterile glass coverslips, fed with ACM, and patch-clamped 2 days after isolation.

Reverse Transcriptase-PCR—Reverse transcriptase-PCR was performed as described previously (22). Briefly, total RNA was isolated using TRIZOL reagent (Invitrogen) from cultures that were >98% pure microglia. To eliminate genomic contamination, the cell suspension was digested with DNase I (Amersham Biosciences) at 0.1 units/ml, for 15 min at 37 °C. First strand cDNA was synthesized using an oligo(dT) primer (Amersham Biosciences) and used as a template for PCR reactions with a gene-specific primer (from ACGT, Toronto, ON) for ChaK (GenBank™ accession number NM_053705) (forward primer CTGAAGAGGAATGACTACAC; reverse primer ACAGGGAAAAAGAGAGGGAG). As a control, oligo mouse actin (M12481) was amplified (forward primer CTACAATGAGCTGCGTGTGG; reverse primer TAGCTCTTCTCCAGGGAGGA). The PCR reaction was conducted with 1.5 mM $MgCl_2$, 0.5 μM forward and reverse primers, 10% of the cDNA reaction mixture, and 1.25 μM of *Taq* DNA polymerase, using a GeneAmp PCR 2400 system (PerkinElmer Life Sciences). The mixture was preheated to 95 °C for 5 min and then subjected to 25 cycles of a denaturing phase at 94 °C, a 30-s annealing phase at 55 °C, and a 30-s extension phase at 72 °C. The amplified products were resolved in 2% agarose gels containing 0.5 mg/ml ethidium bromide. The identities of products of the predicted sizes were confirmed by restriction endonuclease digestion.

Patch Clamp Recordings—We made whole-cell or perforated-patch configurations at room temperature with an Axopatch 200A or Axopatch 1B amplifier (Axon Instruments, Union City, CA) and 5–10-megohm resistance pipettes pulled from thick-walled borosilicate glass capillaries (WPI, Sarasota, FL). Capacitance and series resistance (but not leak current) were compensated online, and recordings were filtered at 5 kHz before acquiring data. pCLAMP v6.0 or 8.0 (Axon Instruments) was used for generating voltage commands, recording current, and collecting data, which were analyzed offline with Origin v6.0 (Northampton, MA). Liquid junction potentials were measured between each bath and pipette solution with a 3 M KCl electrode, subtracted offline, and used to correct all voltages and current *versus* voltage relations.

Several combinations of bath and pipette solutions (indicated in each figure legend) were used to isolate the current and to characterize its selectivity and ion dependence. The standard bath solution contained (in mM) 125 NaCl, 5 KCl, 1 $CaCl_2$, 1 $MgCl_2$ and 10 HEPES, and standard pipette solution contained 40 KCl, 100 potassium aspartate, 1 $MgCl_2$, 1 $CaCl_2$, 10 HEPES, 2 K_2ATP, and 10 EGTA. To minimize contributions of the swelling-activated Cl^- current (20) many experiments were performed with low Cl^- solutions made by substituting NaCl and KCl with 125 mM $NaMeSO_4$ and 5 mM $KMeSO_4$ (bath) and 130 mM $KMeSO_4$ or potassium aspartate (pipette). Sucrose was added when necessary to adjust the osmolarity of all solutions to 300 milliosmolar, measured with a freezing point-depression osmometer (Advanced Instruments, Norwood, MA). For ion-selectivity studies, low Cl^- solutions were used, with one of the following substitutions: 130 mM nMDG $MeSO_4$ (pipette), K^+-free bath, or pipette solutions were made by replacing KMeSO4 with $CsMeSO_4$, or a divalent-free bath solution was prepared by replacing $MgCl_2$ and $CaCl_2$ with 4 mM NaCl and adding 10 mM HEDTA. To assess the dependence of the current on internal Ca^{2+}, the pipette calcium solutions contained 1 mM $K_4$1,2-bis(2-aminophenoxy) ethane *N*,*N*,*N*′,*N*′-tetraacetic acid (K_4BAPTA) instead of EGTA, with free Ca^{2+} adjusted by adding $CaCl_2$, according to the CaBuffer program (from J. Kleinschmidt, formerly of New York University). The effect of changing the internal Mg^{2+} concentration was tested by adding $MgCl_2$ to the low Cl^- pipette solution while keeping the ATP concentration fixed at 2 mM. For perforated-patch recordings, the pipette was back-filled with intracellular solution containing 20 μg/ml amphotericin B (Sigma) diluted from a freshly prepared 1 mg/ml stock solution in Me_2SO (23). All bath solutions were pH 7.4 (adjusted with NaOH), and pipette solutions were pH 7.2 (adjusted with KOH or CsOH).

To initially assess regulation of the current by tyrosine kinases, a broad-spectrum tyrosine kinase inhibitor, genistein (or its inactive analogue, daidzein, both at 50 μM), or the more Src-selective inhibitor, herbimycin A (2 μM) (24) (all from Sigma), was added to the bath. A specific role for Src tyrosine kinase was further examined using pipette solutions containing the Src peptide, Src40–58, or the scrambled inactive peptide, Src40–58s (0.1 mg/ml), as we described previously (25, 26). The peptides were synthesized at the Hospital for Sick Children (Toronto). Spermine was purchased from Calbiochem, and unless indicated, the remaining chemicals were purchased from Sigma and were the highest purity available.

Statistics—Where appropriate, data are presented as mean ± S.E., with *n* indicating the number of cells studied under each condition. Differences between means were analyzed by using either paired or unpaired Student's *t* tests as appropriate.

RESULTS

Biophysical Properties of the TRPM7-like Current in Rat Microglia

An Outward-rectifying Cation Current—Unless otherwise indicated, all recordings were from microglia that were cultured in serum-free medium or astrocyte-conditioned medium, conditions that reduce microglia activation (21). We patch-clamped microglia that were unipolar or bipolar with elongated cell bodies, as in one of our earlier studies (12). Throughout this study, the holding potential was −5 mV to inactivate the voltage-gated K^+ currents that have been well characterized in microglia: Kv1.3-like (12, 25, 27) and Kv1.5-like currents (12). Voltage-clamp steps and ramps were applied between −85 and +115 mV, avoiding more negative potentials that activate the well characterized inward rectifier (Kir2.1-like) current (20, 27). Except where noted, we observed an outward rectifying current that lacked time-dependent activation or inactivation during voltage-clamp steps. Fig. 1, *A* and *B* shows examples of the current; similar currents were seen in >200 microglia and, as shown in subsequent figures, under a wide range of conditions. Responses to voltage steps and ramps illustrate some hallmarks of this current; that is, lack of detectable time-dependent gating and strong outward rectification with a reversal potential of about −15 mV with standard bath and pipette solutions (*circles* in Fig. 1*C*). These features are very similar to the recently cloned TRPM7 channel (9, 11). Most reports on transfected TRPM7 channels (9, 11) have not shown or mentioned the tail currents, and many have shown currents only in response to voltage-ramp protocols. We found very small tail currents upon return to the holding potential of −5 mV (Fig. 1, *A* and *E*), which was close to the reversal potential. When steps to more negative potentials followed strong depolarizing steps, the tail currents were immediately small (not shown), without the relaxations that occur when voltage-gated channels close with hyperpolarization. A similar lack of time dependence is expected for TRPM7 channels, because the inward current is rapidly blocked by external divalent cations.

The outward current is carried by efflux of monovalent cations. That is, replacing intracellular K^+ with $nMDG^+$ nearly eliminated the outward current (Fig. 1*C*), demonstrating that the monovalent cation, K^+, is highly permeant, but the bulky cation, $nMDG^+$, is not. In contrast, replacing external Cl^- with methanesulfonate ($MeSO_4$) (Fig. 1*D*) did not affect the current amplitude or rectification, and similar results were seen with external aspartate (n = 3 cells, not shown). Thus, the outward current is not because of anion influx. K^+ appears to be more permeant than Cs^+, because the outward current was significantly reduced by replacing internal K^+ with Cs^+ (Fig. 1*C*). Although a selectivity sequence of $K^+ > Cs^+ > nMDG^+$ is characteristic of K^+ channels, the reversal potential of −10 to −15 mV with internal K^+ or Cs^+ rules out a K^+-selective channel; E_K is −85 mV with the normal K^+-containing bath and pipette solutions used in Fig. 1, *A–C*. However, these features are typical of the TRPM7 channel, which passes monovalent cations (not anions) with a permeability sequence $K^+ \sim Cs^+ \sim Na^+ > Ca^{2+}$ (9). Possible contributions of ionotropic purinergic receptors, which produce a non-selective cation current in microglia (see "Discussion"), were ruled out by several observations. First, to eliminate the possibility that ATP leaking from the pipette during seal formation activated the cation current, some experiments were done without ATP; the current activated normally (n = 4, not shown). Second, the outward-rectifying current took several minutes to fully activate (see Fig. 7) whereas purinergic currents activate rapidly in the presence of ATP. Third, purinergic-receptor-mediated currents in microglia have nearly linear I-V relations, with substantial inward current.

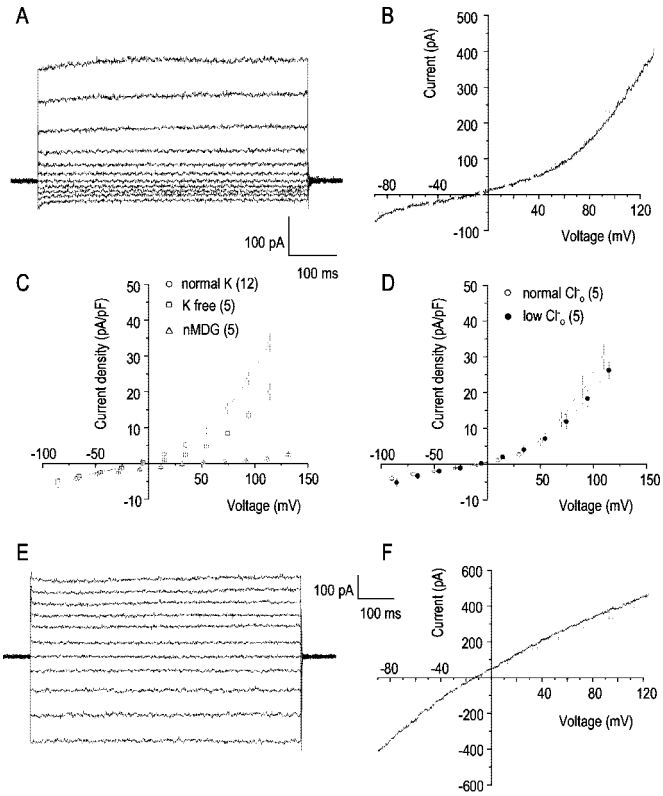

FIG. 1. **Basic biophysical features of the outward-rectifying cation current.** *A*, representative family of currents in response to voltage-clamp steps between −85 and +115 mV in 20 mV increments, from a holding potential of −5 mV (all voltages have been corrected for measured junction potentials). The bath and pipette contained low Cl^- solutions (in mM) as follows: bath solution, 125 $NaMeSO_4$, 5 K $MeSO_4$, 1 $CaCl_2$, 1 $MgCl_2$, 10 HEPES; pipette solution, 130 $KMeSO_4$, 1 $MgCl_2$, 1 $CaCl_2$, 10 HEPES, 2 K_2ATP, 10 EGTA. *B*, same cell as in *A*. Representative current *versus* voltage (I-V) curve produced by a voltage ramp from −85 and +115 mV (holding potential of −5 mV) with the currents from the voltage steps in *A* superimposed (*open circles*). *C*, the outward current is carried by monovalent cations. To normalize for differences in cell sizes, each current has been divided by the cell capacitance to yield the current density (pA/pF). Current density *versus* voltage relations are shown with internal 130 mM $KMeSO_4$ (*circles*), $CsMeSO_4$ (*squares*), or nMDGCl (*triangles*), and external 5 mM $KMeSO_4$ (*circles or triangles*) or 5 mM $CsMeSO_4$ (*squares*). Values are mean ± S.E. for the number of cells indicated in *parentheses*. *D*, the outward current is not carried by anion influx. With standard bath and pipette solutions (see "Experimental Procedures") the current density *versus* voltage relation was outwardly rectifying (*open circles*) and very similar to that in *C*. Replacing the 130 mM Cl^- in the bath and pipette with $MeSO_4^-$ (*closed circles*) did not affect the current amplitude or its outward rectification. Values are mean ± S.E. for the number of cells indicated. *E* and *F*, in the absence of external divalent ions, there was substantial inward current. Representative currents are shown in response to voltage steps (*E*) or a voltage ramp (*F*), with the current amplitudes from voltage steps superimposed (*circles*) (see Fig. 8*C* for average currents in divalent-free solution). The bath and pipette contained low Cl^- solutions, except that $MgCl_2$ and $CaCl_2$ in the bath were replaced with 4 mM NaCl.

In the absence of external divalent cations, a large inward current was revealed during voltage-clamp steps (Fig. 1*E*) or ramps (Fig. 1*F*). As before, there was no time-dependent gating evident, thus the step-elicited currents were superimposed on the ramp currents. As shown here and in Fig. 8*C* (*open circles*), in divalent-free solution there was a dramatic decrease in current rectification; *e.g.* the ratio of current density at +115 mV *versus* −85 mV decreased from 8.6 ± 2.3 in standard bath solution to 1.8 ± 0.3 (n = 7) in divalent-free bath solution. In divalent-free bath solution, the current reversed at −11 ± 1 mV (n = 7), which expected for a non-selective cation channel through which Na^+ (predominant in the bath) and K^+ (predominant in the pipette) permeate well. That is, the K^+ Nernst

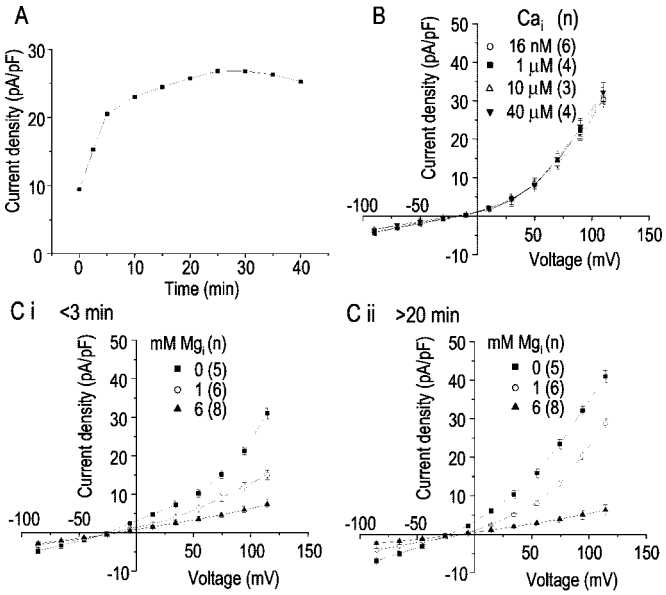

FIG. 2. **Internal Mg^{2+} but not Ca^{2+} inhibits the TRPM7-like current.** *A*, a representative time course of current activation in normal solutions; *i.e.* with 1 mM internal Mg^{2+}. The current density (pA/pF) at +115 mV is shown as a function of time. *B*, the current was not sensitive to large changes in internal Ca^{2+}. The mean current density (pA/pF) *versus* voltage relation is shown. The bath solution contained (in mM) 145 sodium aspartate, 5 KCl, 1 $MgCl_2$, 1 $CaCl_2$, 5 HEPES, and the pipette contained 140 K aspartate, 1 K_4BAPTA, 1 $MgCl_2$, 5 HEPES. Free internal Ca^{2+} was adjusted as indicated by changing the $CaCl_2$ concentration in the pipette solution. Values are mean ± S.E. of the number of cells indicated in *parentheses*. *C*, the mean current density *versus* voltage relation is shown within the first 3 min after break-in (*i*), and 20–23 min later in the same cells (*ii*). Values are mean ± S.E. of the number of cells indicated in *parentheses*. To minimize Cl^- currents, the bath contained 125 mM $NaMeSO_4$ solution, and the pipette contained 130 mM $KMeSO_4$ solution, with Mg^{2+} adjusted by adding $MgSO_4$.

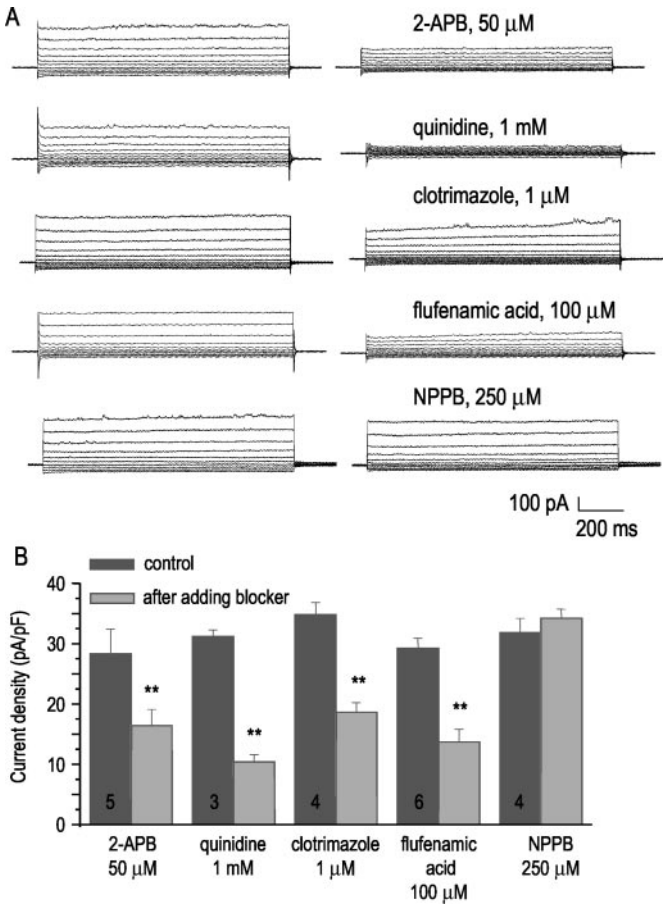

FIG. 3. **Pharmacological properties of the TRPM7-like current.** *A*, representative families of currents in control solutions (*left traces*) and with each blocker (*right traces*) in low Cl^- solutions. For each set of experiments, control currents were recorded for 20 min and then a blocker was perfused into the bath, and currents were recorded again after 5 min; *i.e.* much longer than it took for the degree of block to stabilize. *B*, summary of the average current density at +115 mV with and without each blocker. Values are mean ± S.E., for the number of cells indicated on each control *bar* (**, $p < 0.001$ paired Student's *t* test).

potential is about −85, and the Na^+ Nernst potential is about +60 mV; thus, if the TRPM7 channel is equally permeable to K^+ and Na^+ (9) the reversal potential should be ~−12 mV.

Inhibition by Intracellular Mg^{2+} but Not by Intracellular Ca^{2+}—With the standard 1 mM Mg^{2+} and 2 mM K_2ATP in the pipette, the outward-rectifying current increased over the first several minutes of whole-cell recording (Fig. 2*A*; for average time course see Fig. 7*D*). The current was not sensitive to internal Ca^{2+} (Fig. 2*B*); *i.e.* there were no changes in current density, degree of outward-rectification, or reversal potential over a wide range of free Ca^{2+} concentrations. Thus, the microglia channel is not Ca^{2+}-activated, like some cation nonselective channels (28, 29), or subject to Ca^{2+}-dependent slow deactivation, as is the CRAC current (30). Consistent with our results, buffering internal Ca^{2+} to ~100 nM had no effect on cloned TRPM7 channels (31). However, there was a dose-dependent inhibition of current by internal Mg^{2+}. The current density at both early (<3 min; see Fig. 2*C*, *part i*) and later times (>20 min; see Fig. 2*C*, *part ii*) reached significantly larger values when internal Mg^{2+} was omitted. In contrast, the normal time-dependent build up of current was essentially prevented by 6 mM internal Mg^{2+}, a concentration found previously (11) to fully inhibit cloned TRPM7 channels. The free concentrations of Mg^{2+} (calculated with the CaBuffer program and taking into account 2 mM ATP) were 73 μM when total Mg^{2+} was 1 mM and 2.8 mM when total Mg^{2+} was 6 mM. Normal free Mg^{2+} levels in mammalian cells are 0.25–1 mM (32, 33). Although increasing total Mg^{2+} reduces ATP availability, this cannot account for the changes in current, because we observed current run-up without ATP in the pipette solution ($n = 4$, data not shown). The observed inhibition of this current by millimolar intracellular Mg^{2+} is consistent with cloned TRPM7 and native TRPM7-like channels in other cells (3–5, 10, 11, 19). Although the reversal potentials (E_{rev}) were similar upon break-in, after 20–23 min E_{rev} values were about −10 mV with 1 and 6 mM Mg^{2+} compared with −23 mV with 0 mM internal Mg^{2+}. One possibility is that reduced block by internal Mg^{2+} allowed more monovalent current to flow, seen as a larger inward current.

Pharmacological Properties of the TRPM7-like Current

We tested several ion-channel blockers (Fig. 3), focusing on a known inhibitor of TRPM7 channels, 2-aminoethyldiphenyl borate (2-APB), a rather non-selective cation channel blocker (quinidine), and known blockers of other ion channels in microglia: SKF-96365, clotrimazole, flufenamic acid, and 5-nitro-2-(3-phenylpropylamino)benzoic acid (NPPB). In each case, the drug concentration chosen was higher than the K_d or IC_{50} for block of the relevant channel, and different cells were used for each test. To minimize Cl^- currents, low Cl^- bath and pipette solutions were used. Effects of the drugs could not be attributed to current run-down, because in time-matched control recordings there was no run-down by 30 min, the longest time used for drug treatments. Drug reversibility was not fully assessed, but all were at least partly reversed during a 2–3-min washing period. The TRPM7 blocker, 50 μM 2-APB (3, 5), significantly inhibited the outward-rectifying current in microglia; *i.e.* by

42% at +110 mV. The ability of the CRAC blocker, SKF-96365, to block TRPM7-like channels is somewhat controversial, with 20 μM producing no block in one study (5) and irreversible block in another (4). We observed no block of the TRPM7-like current by 20 μM SKF-96365 (n = 4, data not shown). The trivalent cations, La^{3+} and Gd^{3+}, which block CRAC channels at micromolar concentrations (3, 34), only reduce cloned or native TRPM7 currents at millimolar concentrations (6, 9, 10). We found about 50% block of the microglial current by 1–2 mM La^{3+} (n = 3, not shown). Quinidine (1 mM) reduced the outward-rectifying current by 67%. However, quinidine is not very selective at such high concentrations but also blocks some sodium channels (35), Kv (36), and non-selective cation channels (37). Clotrimazole blocks the Ca^{2+}/calmodulin-activated K^+ channel, SK4, in microglia (13, 38) and other cells, with a K_d of about 25 nM (22, 39). It is intriguing that the TRPM7-like current in microglia was reduced by 47% by 1 μM clotrimazole. This cannot be attributed to contamination by SK4 channels, because the current was not K^+-selective (Fig. 1*C*) and was completely insensitive to changes in internal Ca^{2+} (Fig. 2*B*). Flufenamic acid is usually used as a Cl^- channel blocker, and consistent with this finding, the swelling-activated Cl^- current in rat microglia was fully blocked by 100 μM flufenamic acid (20). The same concentration reduced the TRPM7-like current by 53% in the present study (Fig. 3*B*) and inhibited a non-selective cation current in epithelia (37). The lack of specificity of these high concentrations of flufenamic acid, quinidine, and clotrimazole mean that caution is needed in interpreting results of cell-functional studies using these drugs. In contrast, another Cl^- channel blocker, NPPB, which fully blocks the swelling-activated Cl^- current in rat microglia at 250 μM (20), did not affect the TRPM7-like current in these cells (Fig. 3*B*). This result supports the use of NPPB for assessing the roles of Cl^- channels in microglia and verifies that the TRPM7-like outward-rectifying current is not contaminated by Cl^- current in our recordings.

Microglia Express Transcripts for the TRPM7 Channel

Essentially all properties described thus far for the outward-rectifying channel in rat microglia are similar to those of cloned TRPM7 channels (9, 11), reviewed in Refs. 6, 7, and 40. TRPM7 is expressed in a wide range of tissues, including brain, skeletal muscle, kidney, heart, liver, and spleen. Thus, it was not surprising that rat microglia express transcripts for TRPM7 (Fig. 4). These microglia were cultured under the same conditions used for the patch clamp analyses in Figs. 1–7. Because there were no differences in current in response to several activating stimuli (see Fig. 9*B*), we did not assess whether the TRPM7 mRNA level changed with microglia activation.

Regulation of the TRPM7-like Current

Spontaneous Development of the TRPM7-like Current in Whole-cell Recordings—Currents from heterologously expressed TRPM7 channels (9, 11) and native TRPM7-like currents (3–5) spontaneously activate in whole-cell recordings, as did the current in microglia. We showed (Fig. 2*C*) that the current amplitude is more than twice as large with 0 mM internal Mg^{2+} than with 1 mM and much smaller with 6 mM Mg^{2+}. Results in Fig. 5, *A–C* shows that the time course of development also depends on the internal Mg^{2+} concentration. That is, with 1 mM internal Mg^{2+} the current doubled in the first 6–8 min (Fig. 5*B*, and see average for control cells in Fig. 7*D*). When internal Mg^{2+} was omitted (Fig. 5*A*), the current activated more rapidly, taking about 70 s to reach the half-maximal amplitude and attaining a plateau in about 2 min. Conversely, with elevated internal Mg^{2+} (6 mM), the current

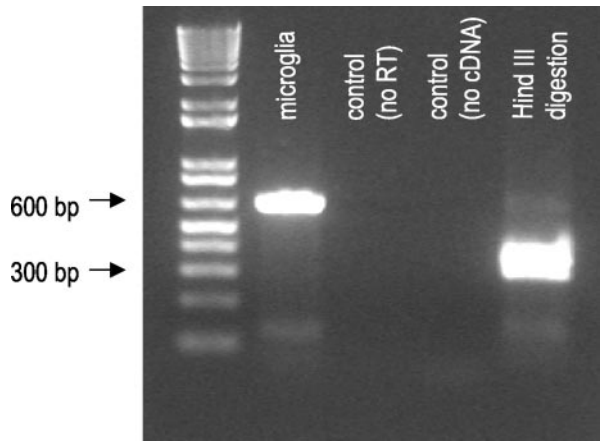

FIG. 4. **TRPM7 transcripts are present in rat microglia.** mRNA was prepared from cultured microglia (see "Experimental Procedures"). TRPM7-specific forward and reverse primers amplified a product of the correct size (*lane 2*) but not in the negative controls when either reverse transcriptase or cDNA was omitted (*lanes 3* and *4*). Restriction enzyme digestion (*lane 5*) produced two products of the expected sizes (306, 354 bp), which appear as a *broad band*.

progressively decreased to about 60% of the initial value by 3 min after establishing a whole-cell recording. Again, half of this decrease was achieved in about 70 s. By plotting both inward and outward currents as percent of their peak values, we demonstrate the simultaneous changes in inward and outward currents at each Mg^{2+} concentration, further evidence that the same channel carries both currents and that the effects of internal Mg^{2+} on the time course are not voltage-dependent.

In whole-cell recordings, significant current was present immediately after break-in (*e.g.* see Fig. 2*C*, Fig. 5, *A–C*, and Fig. 7, *A* and *D*). However, in perforated-patch recordings there was very little increase in current (Fig. 5*D*, *closed circles*); the average current density after 20 min of recording was 5.4 ± 1.2 pA/pF at +115 mV. Compare this with the 6-fold increase in current density during whole-cell recordings with 1 mM total Mg^{2+} (*open circles*). Current development during whole-cell recordings produced a stable, activated state. That is, for two cells, the current was allowed to develop during a whole-cell recording and then the pipette was removed (not shown). When a second whole-cell recording was established on the same cells, the current was immediately large. This observation, and the spontaneous development of current in whole-cell but not perforated-patch recordings, suggests that the TRPM7-like current is activated by washout of an intracellular inhibitor. Cell swelling activates a pronounced Cl^- current in microglia, which is blocked by NPPB (see Fig. 5*E* and Ref. 20) However, activation of the TRPM7-like current could not be attributed to changes in cell volume during whole-cell recording, because the current was not affected by a hypotonic bath solution (Fig. 5*E*).

Spermine Blocks the TRPM7-like Current in a Voltage-dependent Manner—Another characteristic of TRPM7 channels is their block by external polyvalent cations like spermine and spermidine. This block is voltage-dependent, with more block of inward currents at moderately negative potentials that help to drive the polyvalent cations into the external pore. A detailed study (41) of native TRPM7-like channels in rat basophilic leukemia cells showed some relief of block at strongly hyperpolarized potentials that drive the external polyvalent cations through the channel. In addition, they observed some block of outward current at positive membrane potentials when the polyvalent cation concentration was high. Thus, to examine the block by external spermine, we used 0 mM internal Mg^{2+} to allow the current to develop and stabilize quickly (as in Fig. 5*A*) and increased the inward current by perfusing in a divalent

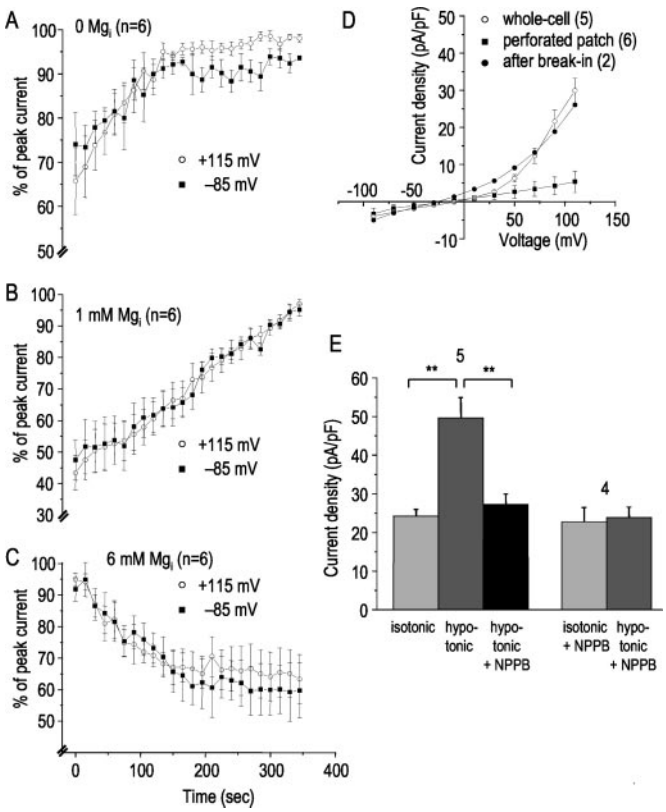

FIG. 5. **Controlled development of the TRPM7-like current.** *A–C*, intracellular Mg^{2+} affects the time course of spontaneous development of the outward current (measured at +115 mV) and inward current (measured at −85 mV). Whole-cell recordings were made with different Mg^{2+} concentrations in low Cl^- solutions (to eliminate Cl^- currents). Before averaging, each point was calculated as a percent of the maximal inward or outward current for each cell, to standardize for different current amplitudes between cells and the much smaller inward than outward currents. Values are mean ± S.E. for the number of cells indicated in *parentheses*. *D*, spontaneous development of the current was markedly reduced in perforated-patch recordings. First, perforated-patch recordings were alternated with whole-cell recordings on different cells, and the average current densities were compared at 20–30 min of recording (by which time whole-cell currents reach steady-state; see Fig. 2*A*). Second, for two cells, perforated-patch recordings were followed by breaking into the whole-cell configuration and recording for a further 20 min (*closed circles*). Values are mean ± S.E. for the number of cells indicated in *parentheses*. *E*, the TRPM7-like current is not sensitive to cell swelling. In control recordings (*three left-hand bars*) with standard bath and pipette solutions, perfusion of a hypotonic solution (75% of normal osmolarity) into the bath activated a swelling-sensitive Cl^- current that was fully blocked by 250 μM NPPB. In separate cells (*right-hand bars*), the TRPM7-like current was allowed to run up in isotonic solution and then 250 μM NPPB was perfused in, followed by the hypotonic solution. There was no increase in the NPPB-insensitive TRPM7-like current. Values are current density at +115 mV, mean ± S.E. for the number of cells indicated *above* each set of *bars*.

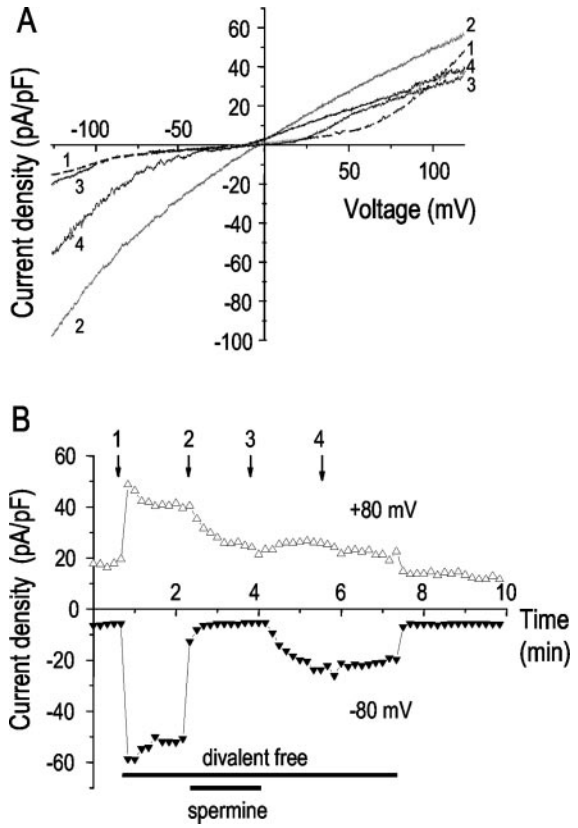

FIG. 6. **Spermine blocks the TRPM7-like current in a voltage-dependent manner.** *A*, a representative cell showing current *versus* voltage curves from ramp voltage-clamp protocols. *Dashed trace* (*labeled 1*) shows control, outward-rectifying current in normal bath solution. *Trace 2* shows larger, slightly inward-rectifying current after divalent cation-free solution was perfused into the bath. *Trace 3* shows reduced current after perfusing 100 μM spermine into the divalent-free bath; note greater reduction of inward current. *Trace 4* shows partial restoration of the current after spermine was washed out of the bath for 4 min. *B*, the time course of the experiment in *A* plotted as outward current at +80 mV and inward current at −80 mV. The *numbers* indicate the times at which the currents in *A* were recorded. After washing out spermine, the normal bath solution (containing divalent cations) was perfused in.

cation-free bath solution (as in Fig. 1*E*). Fig. 6 shows representative current *versus* voltage curves for one cell (*part A*) and the time course of outward current plotted at +80 mV and inward current at −80 mV for the same cell (*part B*). The *numbers* in *part B* indicate times at which the currents in *part A* were recorded. After the current had stabilized in normal bath solution (*trace 1*), divalent-free solution was perfused into the bath, resulting in larger inward and outward currents with little rectification (*trace 2*; compare with Fig. 1*F*). Perfusing spermine (100 μM) into the bath in divalent-free solution essentially abolished the inward current between 0 and −80 mV (leak current remained) and moderately reduced the outward current (*trace 3*). The block was reduced by washing out the spermine for 3–4 min (*trace 4*) before returning to the normal bath solution. Consistent with previous studies, the block was voltage-dependent with an average block of 94.4 ± 5.7% at −80 mV and 41.1 ± 8.2% at +80 mV (n = 4 cells).

Broad-spectrum Tyrosine Kinase Inhibitors Reduce the TRPM7-like Current—For all experiments using protein tyrosine kinase inhibitors, low Cl^- bath and pipette solutions were used to eliminate Cl^- currents. Some outward-rectifying current was present at +115 mV upon break-in; *i.e.* ~30% of the maximal current in this cell. The TRPM7-like current was inhibited rapidly and reversibly by bath addition of the broad-spectrum tyrosine kinase inhibitor, genistein (50 μM) (Fig. 7*A*), with a maximal inhibition of 59 ± 5% (Fig. 7*C*) within 10 min. After washing out genistein, the current recovered fully over the next ~10 min in this cell. The effects of genistein were rapid and reversible in all eight cells tested. Although there is precedent for direct block of some channels by genistein, this is unlikely to be the case for the TRPM7-like current. That is, the time needed to exchange the small bath volume (250 μl) was <30 s, so the several minutes required for onset and recovery of genistein inhibition were not because of the perfusion time. The inactive analogue, daidzein, did not significantly reduce the current (Fig. 7, *A* and *C*). The genistein-sensitive current that was isolated by subtraction (Fig. 7*B*) displayed the typical outward-rectifying profile of TRPM7, with large currents above

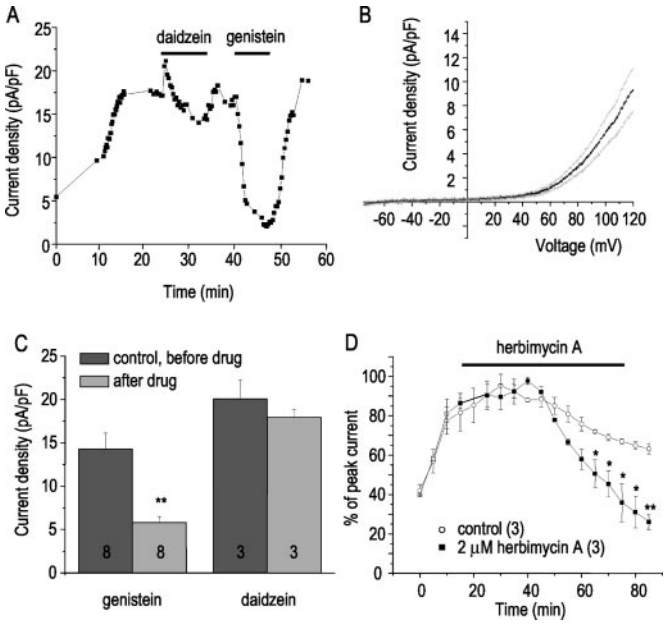

FIG. 7. **Tyrosine kinase inhibitors reduce the TRPM7-like current.** All whole-cell recordings were made with low Cl^- solutions to eliminate Cl^- currents. *A*, genistein inhibits the current. A representative recording, plotted as current density at +115 mV, shows the dramatic and reversible inhibition by genistein but not the inactive analogue, daidzein. After the current developed and stabilized (~20 min after break-in), 50 μM daidzein was perfused into the bath for about 10 min and then washed out. Then, 50 μM genistein was perfused into the bath for about 8 min and then washed out. *B*, isolating the genistein-sensitive current. For each voltage-clamp ramp, the current remaining after adding 50 μM genistein to the bath was subtracted from the control current to isolate the genistein-sensitive component. Then, the mean current density *versus* voltage relation for the eight cells was calculated (*heavy trace*). The *two thin traces* show the range in the current amplitudes at ± 1 S.E. *C*, summary of inhibition by genistein. The current density at +115 mV (mean ± S.E., number of cells indicated on the *bars*) is shown before and ~5 min after adding 50 μM genistein or daidzein to the bath. Student's paired *t* test, **, $p < 0.01$. *D*, the tyrosine kinase inhibitor, herbimycin A, also reduces the current. Whole-cell recordings were begun in control solutions (*open symbols*) and then half of the cells were exposed to 2 μM herbimycin A at 15 min (*closed squares*). Each current was normalized to its maximal value at +115 mV before calculating the mean values as a function of time. Values are mean ± S.E. for the number of cells shown in *parentheses*. Student's unpaired *t* test, *, $p < 0.05$; **, $p < 0.01$.

+40 mV.

Next, we used the more Src-selective inhibitor, herbimycin A (24). To focus on the time course, differences in current amplitude between cells were eliminated by normalizing the current as percent of maximal current at +115 mV in the same cell (Fig. 7*D*). Again, ~40% of the maximal current was present upon break-in. The current spontaneously increased about 2.5-fold over the next 20–30 min and then slowly decreased to about 65% of the maximal value by 90 min of recording. In separate cells, when 2 μM herbimycin A was added to the bath after 15 min of recording, the current significantly decreased, and only 25% remained by 90 min. Washout of herbimycin was too slow to complete during the lifetime of a recording. The inhibition by two chemically distinct tyrosine kinase inhibitors suggests that tyrosine kinases are involved in the activation or maintenance of the current.

Selectively Inhibiting Src Kinase Reduces the TRPM7-like Current—The inhibition by herbimycin A suggested involvement of an Src family kinase. Thus, we exploited a peptide, Src40–58, made from the unique domain of Src. This peptide was originally used to produce a Src-inhibiting antibody, but the peptide itself was found to act like an inhibitor of Src kinase function when added to the patch pipette during whole-cell

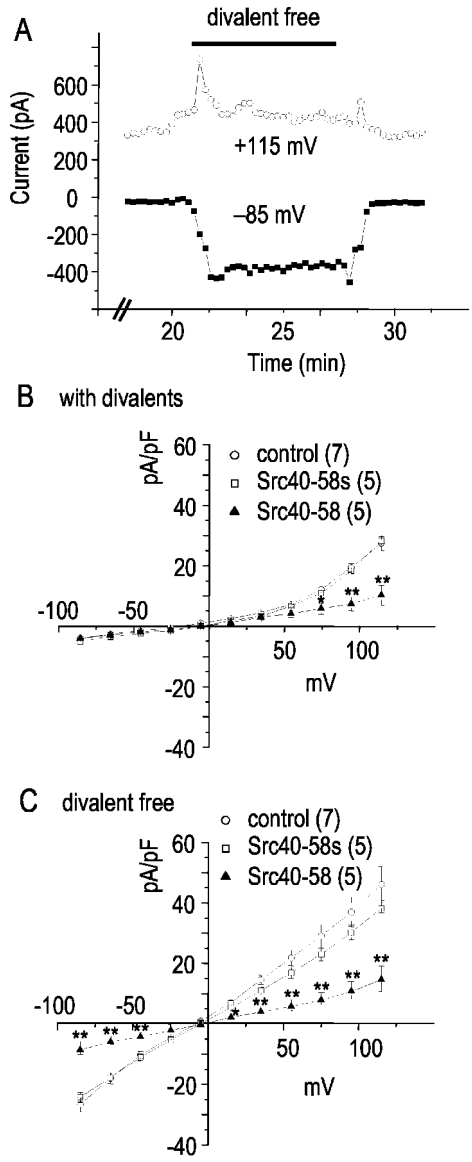

FIG. 8. **Inhibiting Src tyrosine kinase reduces the TRPM7-like current.** All recordings were begun with standard low Cl^- solutions containing 1 mM $CaCl_2$ and 1 mM $MgCl_2$ and then switched for a few minutes to a divalent-free bath solution. *A*, a representative recording of the outward (at +115 mV) and inward (at −85 mV) currents. *B* and *C*, average current density was measured after 20 min of whole-cell recording with standard low Cl^- solutions in the bath and pipette (*control*), with the Src peptide (*Src40–58*, 0.1 mg/ml) or the inactive scrambled peptide (*Src 40–58s*, 0.1 mg/ml) in the pipette solution. In *B*, the bath solution contained 1 mM $CaCl_2$ and 1 mM $MgCl_2$. In *C*, divalent cations were omitted from the bath. Values are mean ± S.E., with the number of cells in *parentheses*; *, $p < 0.05$; **, $p < 0.01$.

recordings (42). Although its precise mechanism of action is still unknown, the authors concluded that the Src40–58 peptide interacts with an unknown protein that regulates Src function (42). Our earlier results are consistent with Src40–58 acting as an Src inhibitor; that is, it produced effects opposite to those of a Src-activating peptide (26). In the present study (Fig. 8), the development of the current was compared with a normal pipette solution or one containing a scrambled version of the Src peptide as a control for the addition of an intracellular peptide. Under control conditions with normal levels of Ca^{2+} and Mg^{2+} in the bath, the outward current increased more than 2-fold within 20 min after break-in ($p < 0.01$, $n = 7$). Perfusing in a divalent-free bath solution revealed the large inward monovalent current (as in Fig. 1, *E* and *F*) but had little

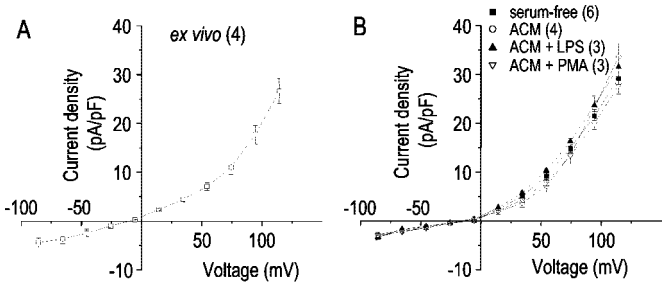

FIG. 9. **The TRPM7-like current is present in microglia at differing activation states.** *A*, whole-cell recordings were made from *ex vivo* microglia; *i.e.* in dissociated brain tissue recorded after only 1 day in culture. Low Cl^- solutions were used in the bath and pipette. The current density (mean ± S.E., $n = 4$) is shown after at least 20 min of recording. *B*, the current density was not affected by culturing conditions or microglia activation. Microglia were grown in serum-free medium or astrocyte-conditioned medium or were treated overnight with the activating agents, 100 ng/ml lipopolysaccharide, or 100 nM phorbol myristate acetate. Values are mean ± S.E. for the number of cells indicated in *parentheses*. Recordings were made with standard solutions (see "Experimental Procedures") wherein the bath contained 125 mM NaCl, and the pipette contained 40 mM KCl and 100 K aspartate.

effect on the outward current. The Src40–58 peptide prevented the spontaneous run-up of the outward-rectifying current, whereas the inactive scrambled peptide had no effect (Fig. 8*B*). Next, a divalent-free bath solution was used to increase the inward current, making it easier to show that the Src peptide simultaneously inhibited both inward and outward currents. In the presence of Src40–58, neither inward nor outward currents ran up even after 20 min, whereas the scrambled peptide had no effect (Fig. 8*C*).

The TRPM7-like Current Is Constitutively Active in Microglia, Regardless of Cell Activation State—The same current was present in microglia recently removed from the brain (see "Experimental Procedures") (Fig. 9*A*) as in cells cultured for nearly 2 weeks (see Figs. 1–8 and Fig. 9*B*). Moreover, the current increased for several minutes after establishing whole-cell recordings, as before, and reached the same average current density. Thus, the expression and activation of TRPM7-like currents are constitutive, not a result of cell-culture conditions. This conclusion is further supported by the lack of difference in current density (Fig. 9*B*) between microglia cultured with serum-free or ACM media, conditions that favor the microglia resting state (21)[2] or cells treated with the activating agents, lipopolysaccharide or phorbol myristate acetate.

DISCUSSION

A TRPM7-like Current in Microglia—Numerous properties of the current we recorded in rat brain microglia are very similar to cloned TRPM7 channels. Heterologously expressed TRPM7 produces a strongly outward-rectifying current, where the outward current is carried by monovalent cations, and the inward current is normally carried by divalent cations, including Ca^{2+} (10, 11). In the absence of external divalent cations, TRPM7 channels are permeable to monovalent cations, and the outward rectification is largely abolished (11). TRPM7 is inhibited by millimolar concentrations of intracellular Mg^{2+} or Mg_2ATP (11). For native TRPM7-like currents, it is often difficult to see an inward Ca^{2+} current, because the whole-cell current is much smaller than for heterologously expressed channels. Thus, Ca^{2+} permeability has been convincingly demonstrated only for transfected TRPM7 (10, 11), where expressed currents were >10 times larger (2–3 nA) than the native current we observed in microglia (~200 pA at +80 mV). The small amplitude of the native TRPM7-like current in microglia also rules out a precise measurement of its reversal potential, especially in divalent-containing solutions (*e.g.* in Fig. 1, *B-D* and Fig. 2) where the very small inward current can include some leak current caused by the patch pipette. In every way we examined, the microglial current is similar to TRPM7. There was (i) a spontaneous increase in current over several minutes during whole-cell recordings, (ii) strong outward rectification above ~+50 mV, (iii) low selectivity among small monovalent cations and a permeability sequence of $K^+ \sim Cs^+ > nMDG^+$, (iv) no discernable permeability to Cl^-, aspartate, or methanesulfonate, (v) a small inward current that was dramatically increased by omitting external divalent cations, (vi) concentration-dependent inhibition by intracellular Mg^{2+} (at 1 and 6 mM total Mg^{2+}), and (vii) inhibition by external 2-APB, La^{3+}, or spermine but not by SKF-96365. The lack of effect of changing intracellular Ca^{2+} (between 16 nM and 40 μM) rules out activation by depletion of Ca^{2+} stores, which is a characteristic of CRAC and TRPC channels. From these properties, it is anticipated that the TRPM7-like current in microglia will mediate a Ca^{2+} influx that increases with hyperpolarization. A role for the outward monovalent cation current is less obvious, but with a depolarized reversal potential (~−15 mV), this channel will also tend to depolarize the cell.

Several compounds commonly used as blockers of other ion channels also inhibited the microglial current. These were quinidine, which is often used as a K^+-channel blocker, clotrimazole, which is usually used to block the Ca^{2+}/calmodulin-gated K^+ channel, SK4 (22, 43, 44), and flufenamic acid, which is usually used to block Cl^- channels (20, 45). There is precedent for quinidine and flufenamic acid blocking a non-selective cation current in epithelia (37).

Channel Regulation—The perplexing question of what activates TRPM7 channels has been investigated using both cloned channels and native TRPM7-like currents. TRPM7 contains an active atypical α kinase domain that was initially thought to be essential for channel activity, because the current was increased by intracellular ATP (9). However, this result has been re-interpreted by several studies showing that the channel is directly inhibited by internal Mg^{2+}, even when it is added with ATP. In fact, high internal Mg^{2+} inhibits in the absence of ATP, and poorly hydrolyzable analogs either do not inhibit (Na·ATPγS) or inhibit in a reversible fashion (Mg·ATPγS) under conditions where channel phosphorylation would have been essentially irreversible (11, 46). Similarly, for native TRPM7-like currents, direct inhibition by Mg^{2+}, rather than ATP or Mg_2ATP, has been clearly demonstrated (19). Some native current has been observed immediately upon establishing a whole-cell recording, and this current progressively declined when internal Mg^{2+} was elevated to several millimolar (see Ref. 4 and present study). With standard or reduced levels of Mg^{2+} in the pipette solution, the TRPM7-like current increased spontaneously for several minutes (see Refs. 9 and 11 and present study). It is notable that, in the current study, when perforated-patch recordings were made from microglia, the initial current was smaller and failed to increase during many minutes of recording, but run-up proceeded normally after the whole-cell configuration was attained in the same cells. Despite the Mg^{2+}-sensitivity of the current, for several reasons we do not think it was activated in whole-cell recordings simply by washout of Mg^{2+}. With 1 mM total Mg^{2+} in the pipette (calculated free Mg^{2+}, 73 μM), the current required 6–8 min for half-activation, much slower than predicted for diffusion of a small ion in a small cell. Moreover, the free Mg^{2+} concentration in intact lymphocytes is 190–290 μM (33), whereas millimolar concentrations are needed to fully block TRPM7 channels (19). Thus, considerable current should have activated in perforat-

[2] R. Jagasia and L. C. Schlichter, unpublished results.

ed-patch recordings if Mg^{2+} was the only cytoplasmic inhibitor. Nor could its activation be explained by the cell swelling that sometimes occurs spontaneously in whole-cell recordings, because the TRPM7-like current was not activated by hypotonic bath solutions. Finally, the microglial current was not activated by changing intracellular ATP, because it did not require ATP in the pipette solution to fully activate. This is in contrast to the swelling-activated Cl^- current in these cells, which requires ATP (20).

The phosphatidylinositol pathway, which couples numerous receptors to phospholipase C (PLC), has been implicated in regulating TRPC3 and TRPC6, which are activated by the PLC product, diacylglycerol or its analogue, 1-deoyl-2-acetyl-sn-glycerol (47, 48). It was initially suspected that TRPM7 might be regulated by the phosphatidylinositol pathway, because it physically interacts with the C2 domain of PLC-b_1 (9), an interaction that was reflected in its previous name, TRP-PLIK ("transient receptor potential-phospholipase interacting kinase"). Because TRPM7 interacts with the C2 domains of PLC-β_1, PLC-β_2, PLC-β_3 (but not PLC-β_4), and PLC-γ_1 (but not PLC-δ_1) (31), differences in PLC-dependent signaling can be expected between different cell types, depending on which PLC isoforms they express, and different receptors, depending on which downstream pathways they use. Receptor-mediated activation of PLC rapidly inhibited, rather than activated, TRPM7 (31). This inhibition appeared to be because of hydrolysis of the PLC substrate, phosphatidylinositol 4,5-bisphosphate, either by heterotrimeric G proteins linked to PLC-β or the receptor tyrosine kinase activation of PLCγ by the epidermal growth factor receptor. It was not because of reduced diacylglycerol production, because inhibition was not prevented by adding the analogues, 1-deoyl-2-acetyl-sn-glycerol or diacylglycerol. Although the epidermal growth factor receptor is a receptor tyrosine kinase, TRPM7 activation was attributed to phosphatidylinositol 4,5-bisphosphate, thus no link has yet been made between TRPM7 and tyrosine phosphorylation.

We have now shown that several inhibitors of tyrosine kinases inhibit the activation of the TRPM7-like current during whole-cell recordings from rat microglia. The inhibitors used ranged from the broad-spectrum genistein to the more Src-selective herbimycin A to the peptide, Src40–58, which prevents Src actions (42). Taken together, our results implicate Src itself in regulating the current but do not rule out the possibility that other protein tyrosine kinases also regulate TRPM7 channels. Further studies on the mechanism of regulation will be needed to address whether Src binds to and phosphorylates a specific tyrosine residue on TRPM7 and whether this residue is responsible for regulating the channel. The effect of inhibitors of protein tyrosine kinase(s) means that the spontaneous activation of current in whole-cell recordings might reflect spontaneous activation of a kinase or conversely, washout or inhibition of a tyrosine phosphatase.

Physiological Perspective—There is considerable interest in identifying Ca^{2+} entry pathways in non-excitable cells, which usually lack voltage-gated Ca^{2+} channels. Although it was initially thought that small-conductance CRAC channels provide this pathway, the more recently identified TRPM7 channels are very likely to be important (40). TRPM7-like currents have been identified in a number of non-excitable cells. Because of their Ca^{2+} permeability and lack of voltage-dependent gating they are well designed to contribute to numerous Ca^{2+}-dependent cell processes, which in immune cells include responses to mitogens, secretion of cytokines, lymphokines and antibodies, phagocytosis, and the concomitant respiratory burst. To accurately compare the contribution of TRPM7 with that of CRAC or other store-operated Ca^{2+} channels, it will be important to develop potent and selective blockers. Although antisense knockdown is another potential approach, it may be problematic, because the level of TRPM7 activity appears to control cell survival. That is, targeted deletion in a chicken B-cell line induced growth arrest and cell death, and overexpression killed HEK cells within 24 h (11). If endogenous TRPM7 activity is tightly regulated, one possibility is that large changes in these currents cause cell death under pathological conditions. Although TRPM7 channels will likely respond to tissue ischemia, an expected and direct outcome should be a decrease in current, because the channels are inhibited by high internal free Mg^{2+} (19). Intracellular ATP is a major buffer of Mg^{2+} in mammalian cells (33), thus when it is depleted following severe metabolic disruption, as in ischemia, free Mg^{2+} can rise substantially (33, 49). This should inhibit TRPM7 channels, an effect that should be exacerbated by Mg^{2+} permeation. TRPM7 channels are more permeable to Mg^{2+} than Ca^{2+} and have a permeability sequence of $Zn^{2+} \sim Ni^{2+} \gg Ba^{2+} > Co^{2+} > Mg^{2+}$ Mn^{2+} Sr^{2+} Cd^{2+} Ca^{2+} (10). This unusual permeability raises the possibility that these channels can regulate cellular levels of essential metal ions (*e.g.* Mg^{2+}, Mn^{2+}, Co^{2+}). However, the conjecture that TRPM7 channels allow toxic heavy metals to enter cells and kill them (10) is challenged by the observation that high intracellular levels of these divalent cations inhibit TRPM7-like current (19).

Our observation that inward and outward TRPM7-like currents are reduced by inhibiting the widely expressed Src tyrosine kinase could have profound implications for cell physiology, for instance of microglia. As the resident macrophages of the central nervous system, microglia play important roles in maintaining brain functions. In response to nearly every central nervous system insult (damage or disease), microglia transition from resting to activated states, which exhibit both beneficial and deleterious properties. Microglial activation is not an all-or-nothing response but appears to be a graded phenomenon. It includes some, but not necessarily all, of the following: proliferation, migration to the site of injury, phagocytosis and respiratory burst, synthesis of major histocompatibility complex molecules and antigen presentation, and morphological changes. Some of these changes are accompanied by release of potentially cytotoxic substances (*e.g.* reactive oxygen intermediates, nitric oxide, excitatory amino acids, proteases) or neurotrophic molecules, growth factors, and inflammatory cytokines (*e.g.* interleukin-1, interferon γ, transforming growth factor-β) (50–53).

Studies of the roles of ion channels in microglia activation are at an early stage. Nevertheless, voltage-gated K^+ (Kv) channels and swelling-sensitive Cl^- channels appear to be important for proliferation (12, 20), and the respiratory burst involves Kv1.3 and Ca^{2+}/calmodulin-dependent K^+ (SK3 and SK4) channels (13). The current model for the mechanism is that K^+ channels hyperpolarize the microglia and enhance Ca^{2+} entry though non-voltage-gated Ca^{2+} channels. Moreover, activation of SK channels requires a rise in intracellular Ca^{2+} and ATP-induced microglial activation, which includes release of TNF-α, plasminogen and cytokines, and is Ca^{2+}-dependent (54). Based on its expression and properties, the TRPM7 channel provides a likely pathway for this Ca^{2+} entry. Numerous receptors expressed in microglia are functionally coupled to Src family tyrosine kinases (55–57); *e.g.* CSF-1R (linked to Src, Fyn, Yes), GM-CSF-R (linked to Lyn, Yes, Hck), Fcγ receptors (Lyn), TNF-αR (Fgr), IL-6R (Hck), and G protein-coupled receptors (*e.g.* for thrombin and PAF). Syk, which is downstream of Src family protein tyrosine kinases, tyrosine-phosphorylates other effectors, including PLCγ. Our present

results on tyrosine kinase-dependent regulation of the TRPM7-like current in microglia means that any of these receptor-mediated pathways could, in principle, provide positive feedback wherein TRPM7 activation and concomitant Ca^{2+} entry further enhances the cellular response.

Acknowledgments—We are grateful to X.-P. Zhu for excellent technical assistance.

REFERENCES

1. Parekh, A. B., and Penner, R. (1997) *Physiol. Rev.* **77,** 901–930
2. Lewis, R. S. (1999) *Adv. Second Messenger Phosphoprotein Res.* **33,** 279–307
3. Hermosura, M. C., Monteilh-Zoller, M. K., Scharenberg, A. M., Penner, R., and Fleig, A. (2002) *J. Physiol* **539,** 445–458
4. Kozak, J. A., Kerschbaum, H. H., and Cahalan, M. D. (2002) *J. Gen. Physiol* **120,** 221–235
5. Prakriya, M., and Lewis, R. S. (2002) *J. Gen. Physiol* **119,** 487–507
6. Clapham, D. E., Runnels, L. W., and Strubing, C. (2001) *Nat. Rev. Neurosci.* **2,** 387–396
7. Montell, C., Birnbaumer, L., and Flockerzi, V. (2002) *Cell* **108,** 595–598
8. Montell, C., Birnbaumer, L., Flockerzi, V., Bindels, R. J., Bruford, E. A., Caterina, M. J., Clapham, D. E., Harteneck, C., Heller, S., Julius, D., Kojima, I., Mori, Y., Penner, R., Prawitt, D., Scharenberg, A. M., Schultz, G., Shimizu, N., and Zhu, M. X. (2002) *Mol. Cell* **9,** 229–231
9. Runnels, L. W., Yue, L., and Clapham, D. E. (2001) *Science* **291,** 1043–1047
10. Monteilh-Zoller, M. K., Hermosura, M. C., Nadler, M. J., Scharenberg, A. M., Penner, R., and Fleig, A. (2003) *J. Gen. Physiol* **121,** 49–60
11. Nadler, M. J., Hermosura, M. C., Inabe, K., Perraud, A. L., Zhu, Q., Stokes, A. J., Kurosaki, T., Kinet, J. P., Penner, R., Scharenberg, A. M., and Fleig, A. (2001) *Nature* **411,** 590–595
12. Kotecha, S. A., and Schlichter, L. C. (1999) *J. Neurosci.* **19,** 10680–10693
13. Khanna, R., Roy, L., Zhu, X., and Schlichter, L. C. (2001) *Am. J. Physiol. Cell Physiol.* **280,** C796–C806
14. Schlichter, L. C., and Khanna, R. (2002) in *Potassium Channels and Proliferation of Neuroimmune Cells* (Rouzaire-Dubois, B., Benoit, E., and Dubrois, J. M., eds) Research Signpost, Trivandrum, Kerala, India
15. Lewis, R. S. (2001) *Annu. Rev. Immunol.* **19,** 497–521
16. Illes, P., Norenberg, W., and Gebicke-Haerter, P. J. (1996) *Neurochem. Int.* **29,** 13–24
17. Hahn, J., Jung, W., Kim, N., Uhm, D. Y., and Chung, S. (2000) *Glia* **31,** 118–124
18. Colton, C. A., Jia, M., Li, M. X., and Gilbert, D. L. (1994) *Am. J. Physiol.* **266,** C1650–C1655
19. Kozak, J. A., and Cahalan, M. D. (2003) *Biophys. J.* **84,** 922–927
20. Schlichter, L. C., Sakellaropoulos, G., Ballyk, B., Pennefather, P. S., and Phipps, D. J. (1996) *Glia* **17,** 225–236
21. Eder, C., Schilling, T., Heinemann, U., Haas, D., Hailer, N., and Nitsch, R. (1999) *Eur. J. Neurosci.* **11,** 4251–4261
22. Khanna, R., Chang, M. C., Joiner, W. J., Kaczmarek, L. K., and Schlichter, L. C. (1999) *J. Biol. Chem.* **274,** 14838–14849
23. Rae, J., Cooper, K., Gates, P., and Watsky, M. (1991) *J. Neurosci. Methods* **37,** 15–26
24. Fujishima, H., Nakano, S., Tatsumoto, T., Masumoto, N., and Niho, Y. (1998) *Int. J. Cancer* **76,** 423–429
25. Cayabyab, F. S., Khanna, R., Jones, O. T., and Schlichter, L. C. (2000) *Eur. J. Neurosci.* **12,** 1949–1960
26. Cayabyab, F. S., and Schlichter, L. C. (2002) *J. Biol. Chem.* **277,** 13673–13681
27. Schilling, T., Quandt, F. N., Cherny, V. V., Zhou, W., Heinemann, U., DeCoursey, T. E., and Eder, C. (2000) *Am. J. Physiol. Cell Physiol.* **279,** C1123–C1134
28. Colquhoun, D., Neher, E., Reuter, H., and Stevens, C. F. (1981) *Nature* **294,** 752–754
29. Petersen, O. H. (2002) *Biol. Res.* **35,** 177–182
30. Zweifach, A., and Lewis, R. S. (1995) *J. Gen. Physiol* **105,** 209–226
31. Runnels, L. W., Yue, L., and Clapham, D. E. (2002) *Nat. Cell Biol.* **4,** 329–336
32. Romani, A. M., and Scarpa, A. (2000) *Front Biosci.* **5,** D720-D734
33. Grubbs, R. D. (2002) *Biometals* **15,** 251–259
34. Aussel, C., Marhaba, R., Pelassy, C., and Breittmayer, J. P. (1996) *Biochem. J.* **313,** 909–913
35. Kodama, I., Toyama, J., Takanaka, C., and Yamada, K. (1987) *J. Mol. Cell Cardiol.* **19,** 367–377
36. Attali, B., Wang, N., Kolot, A., Sobko, A., Cherepanov, V., and Soliven, B. (1997) *J. Neurosci.* **17,** 8234–8245
37. Watsky, M. A. (1995) *Am. J. Physiol.* **268,** C1179–C1185
38. Schilling, T., Repp, H., Richter, H., Koschinski, A., Heinemann, U., Dreyer, F., and Eder, C. (2002) *Neuroscience* **109,** 827–835
39. Ishii, T. M., Silvia, C., Hirschberg, B., Bond, C. T., Adelman, J. P., and Maylie, J. (1997) *Proc. Natl. Acad. Sci. U. S. A.* **94,** 11651–11656
40. Clapham, D. E. (2002) *J. Gen. Physiol.* **120,** 217–220
41. Kerschbaum, H. H., Kozak, J. A., and Cahalan, M. D. (2003) *Biophys. J.* **84,** 2293–2305
42. Yu, X. M., Askalan, R., Keil, G. J., and Salter, M. W. (1997) *Science* **275,** 674–678
43. Chandy, K. G., Cahalan, M., Pennington, M., Norton, R. S., Wulff, H., and Gutman, G. A. (2001) *Toxicon* **39,** 1269–1276
44. Jensen, B. S., Strobaek, D., Olesen, S. P., and Christophersen, P. (2001) *Curr. Drug Targets.* **2,** 401–422
45. Schumacher, P. A., Sakellaropoulos, G., Phipps, D. J., and Schlichter, L. C. (1995) *J. Membr. Biol.* **145,** 217–232
46. Perraud, A. L., Fleig, A., Dunn, C. A., Bagley, L. A., Launay, P., Schmitz, C., Stokes, A. J., Zhu, Q., Bessman, M. J., Penner, R., Kinet, J. P., and Scharenberg, A. M. (2001) *Nature* **411,** 595–599
47. Hofmann, T., Obukhov, A. G., Schaefer, M., Harteneck, C., Gudermann, T., and Schultz, G. (1999) *Nature* **397,** 259–263
48. Venkatachalam, K., van Rossum, D. B., Patterson, R. L., Ma, H. T., and Gill, D. L. (2002) *Nat. Cell Biol.* **4,** E263-E272
49. Harman, A. W., Nieminen, A. L., Lemasters, J. J., and Herman, B. (1990) *Biochem. Biophys. Res. Commun.* **170,** 477–483
50. Stoll, G., and Jander, S. (1999) *Prog. Neurobiol.* **58,** 233–247
51. Streit, W. J., Walter, S. A., and Pennell, N. A. (1999) *Prog. Neurobiol.* **57,** 563–581
52. Aloisi, F. (2001) *Glia* **36,** 165–179
53. Inoue, K. (2002) *Glia* **40,** 156–163
54. Hide, I., Tanaka, M., Inoue, A., Nakajima, K., Kohsaka, S., Inoue, K., and Nakata, Y. (2000) *J. Neurochem.* **75,** 965–972
55. Daeron, M. (1997) *Int. Rev. Immunol.* **16,** 1–27
56. Thomas, S. M., and Brugge, J. S. (1997) *Annu. Rev. Cell Dev. Biol.* **13,** 513–609
57. Latour, S., and Veillette, A. (2001) *Curr. Opin. Immunol.* **13,** 299–306